Preparation and photocatalytic hydrogen evolution of g-C_3N_4/ZnO composite

Shenghua Ma* and Wanxi Wang

School of physics and electronic information engineering; Qinghai Nationalities university, Xining, Qinghai, 810007, China

Abstract: The photocatalytic composite of g-C_3N_4/ZnO with different g-C_3N_4 content have been prepared by thermopolymerization method. The catalysts are characterized and analyzed by SEM, XRD, UV-Vis, BET and other analytical methods. The results show that g-C_3N_4/ZnO composites caused the red shift of the absorption band edge of ZnO, which increased the absorption of visible light and the separation rate of photogenerated electron-hole pairs. It is found that the H_2 production rate of 25% g-C_3N_4/ZnO sample is best with 306.25 μmol·h^{-1}·g^{-1}, which is 4.6 times higher than of g-C_3N_4.

1 Introduction

As a high calorific value, pollution-free and renewable clean energy, hydrogen has attracted wide attention. Semiconductor-based photocatalytic hydrogen (H_2) production from water has been considered as one of the effective ways to easing the worldwide energy crisis[1]. ZnO is an n-type semiconductor material, which has been proven to be a promising photocatalyst for environmental applications due to its electric properties, low cost, and non-toxic[2,3]. Nano-sized ZnO has better photocatalytic performance due to surface effect and macroscopic quantum tunneling effect. However, ZnO has a wide band gap of about 3.3 eV and be excited only in a limited ultraviolet region leading to non-responsive in visible light. ZnO is prone to photocorrosion leading to low stability, which has significantly limit the photocatalytic performance [4].

Graphitic carbon nitride (g-C_3N_4) is an attractive nonmetal photocatalyst, which shows excellent performance in the field of hydrogen production from photolysis water[5], photocatalytic degradation of organic compounds[6] and photocatalytic reaction[7] due to its high thermal and chemical stability, small band gap (2.7 eV), low price, easy synthesis method, non-toxicity and high solar energy utilization[8]. In particular, g-C_3N_4 has the characteristic that the composite with other semiconductor materials can expand the light response range of semiconductors, which has become a major research hots pot in the field of photocatalysis. However, due to its low conductivity, low specific surface area and high recombination rate of photoelectrons, the photocatalytic efficiency of g-C_3N_4 is limited[9]. Attempts to combine g-C_3N_4 and other semiconductors have been reported to improve the separation efficiency of photogenerated electron-hole pairs and the photocatalytic performance of g-C_3N_4. Li et al.[10] fabricated a porous g-C_3N_4/TiO_2 heterostructure realizing efficient photoinduced electron−hole separation during photocatalytic process. It degraded acid orange with 82% efficiency after 10 min under simulated solar light, and showed excellent cycle stability. Ge et al.[11] prepared g-C_3N_4/Bi_2WO_6 composite photocatalysts that had a red shift and strong absorption in the visible light region. The photocatalysts exhibit a significantly enhanced photocatalytic performance in degrading methyl orange due to the synergic effect and photo-generated carrier separation.

Microwave solvothermal method is a green and efficient synthesis method. Compared with traditional methods, microwave can penetrate the reaction medium, directly act on the molecules or atoms of the reaction, and excite the high-frequency vibration of polar molecules[12]. The heat needed for the reaction is generated by the way of energy loss to realize the rapid heating of the material as a whole, so as to shorten the reaction time, improve the reaction efficiency and make the particle size of the material more uniform[13]. In this paper, ZnO material was prepared by microwave solvothermal method, ZnO and g-C_3N_4 were compounded to form heterojunction composites. The band gap of ZnO matches the energy level of g-C_3N_4. Electrons in the conduction band of g-C_3N_4 can be easily injected into the conduction band of ZnO, which can effectively separate electron-hole pairs, improve the photocatalytic activity of g-C_3N_4, broaden the light response range of ZnO semiconductors and make the composites respond in the range of visible light[14].

2 Experimental

2.1 Synthesis of ZnO

0.162g of $Zn(NO_3)_2{\cdot}6H_2O$ was dissolved in a mixed solution of 25 mL of triethanolamine and 75 mL of

hzyzmsh@sina.com

deionized water, and dissolved by magnetic stirring. Then it was transferred to a reactor equipped with a microwave hydrothermal reaction parallel instrument, and the temperature was raised to 160℃ for 20 min. After the reaction finished and cooled, the precipitate was collected by centrifugation and washed three times with distilled water and ethanol. Finally, it was placed in a drying oven at 60℃ for 10 h.

2.2 Synthesis of g-C3N4/ZnO

The melamine was placed in a crucible and putted into a muffle furnace. The temperature was raised to 520℃ at a rate of 10℃/min and kept for 4 h. After cooled to room temperature, a yellow g-C_3N_4 powder was obtained and collected. 1 g ZnO and a certain mass fraction of g-C_3N_4 powder were dispersed into methanol solution and stirred by magnetic heating for 2 h until methanol was evaporated. A series of g-C_3N_4/ZnO composites were obtained by calcining the mixed powder in a Ar atmosphere furnace at 500℃ for 2 h.

2.3 Catalyst characterization

The crystal structure of samples were characterized by X-ray diffraction patterns (XRD) on a Bruker D8 advance diffractomer with Cu Kα radiation. The morphology and microstructures of the samples were characterized with scanning electron microscope (SEM) (Zeiss Merlin). The Brunauer-Emmett-Teller (BET) specific surface area and pore size distribution of all the samples were measured through N_2 adsorption/desorption at 77 K using an adsorption instrument (TriStar II 3020). UV-visible diffuse reflectance spectra (UV-vis DRS) of the obtained samples were recorded on a UV-Vis spectrophotometer (UV－3600 Plus, Japan).

2.4 Photocatalytic activity measurements

0.05 g sample was dispersed in a 250 mL quartz reactor, and 100 mL of the 20vol.% triethanolamine solution was used as a sacrificial agent and 1% wt of Pt as a co-catalyst. First, the vacuum was pumped to remove the air, and the light was turned on for photocatalytic H_2 evolution from water splitting after the magnetic agitator was turned on for 30 min. The hydrogen evolved was analysed by a thermal conductivity detector (TCD) gas chromatograph (GC7900). A 1000W Xe lamp equipped with a band-pass filter (420 nm) was used as the light source.

3 Results and discussion

The XRD patterns of the ZnO, g-C_3N_4 and g-C_3N_4/ZnO samples are show in Fig. 1. The distinct diffraction peak of pure g-C_3N_4 at approximately 13° and 27.5° corresponding to the (100) and (002) crystal plane respectively, which is consistent with the standard card (JCPDS 87-1526)[15]. The characteristic peaks of ZnO are in perfect agreement with the standard diffraction pattern of hexagonal wurtzite (JCPDS 36-1451)[16]. Compared with pure ZnO, the peak shape and position of ZnO in g-C_3N_4/ZnO did not change obviously, which indicated that the recombination of g-C_3N_4 could not change the crystal structure of ZnO. When the mass fraction of g-C_3N_4 is low, its characteristic peaks are not obviously. With the increase of the mass fraction of g-C_3N_4 in composites, the intensity of the diffraction peaks gradually increased. In addition, the XRD patterns of all the samples do not show extra diffraction peaks, indicating that the samples have no other impurities and have high purity.

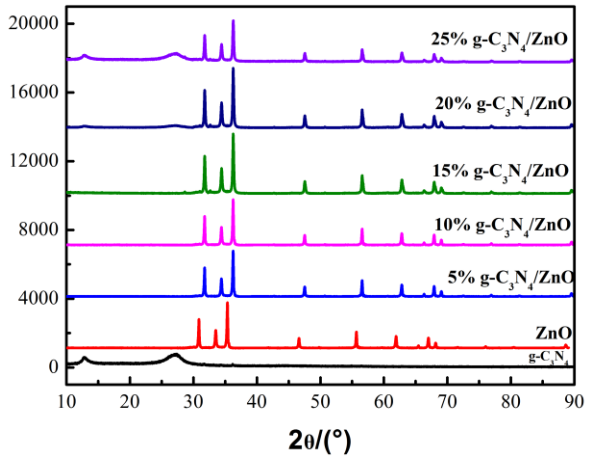

Fig. 1 XRD pattern of the ZnO, g-C_3N_4 and the composites of g-C_3N_4/ZnO.

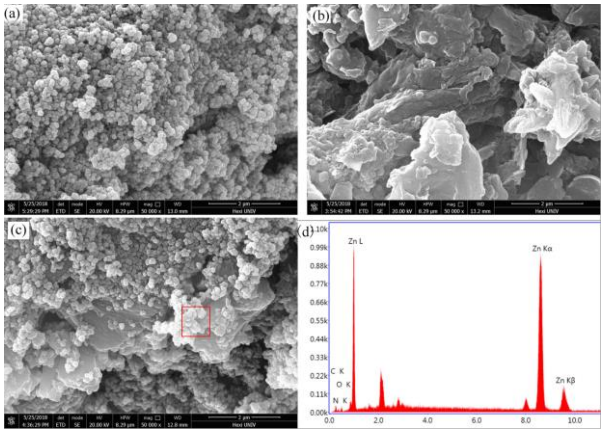

Fig.2 SEM images of the ZnO (a); g-C_3N_4 (b); 25% g-C_3N_4/ZnO (c) and EDS spectrum images of 25% g-C_3N_4/ZnO (d).

As can be seen from the Fig. 2(a), ZnO prepared by microwave solvothermal method is a uniformly distributed nanoparticle microsphere, and the g-C_3N_4 catalyst is formed by stacking with many massive nano-layers that the size is not uniform (Fig. 2(b)), and the ZnO nanospheres in 25% g-C_3N_4/ZnO composits

material are uniformly covered on g-C_3N4 layers (fig. 2(c)). The energy dispersive X-ray spectroscopy (EDX) in Fig. 2(d), resulting from selected area that the sample elements are Zn, O, C and N. Combined with XRD analysis, there are no other impurities in the synthesized g-C_3N_4/ZnO samples, indicating that ZnO is successfully recombined on g-C_3N_4 samples.

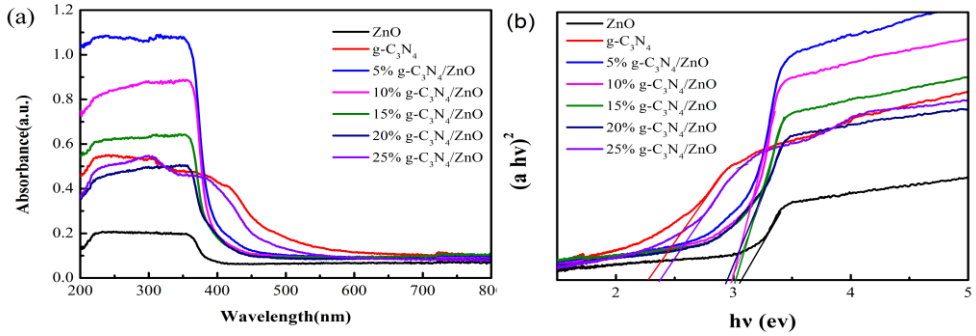

Fig.3 UV-vis diffuse reflectance spectra (a), Tauc plot (b) of ZnO, g-C_3N_4 and the composites of g-C_3N_4/ZnO.

Fig. 3(a) shows the UV-visible diffuse reflection spectra and band gap of g-C_3N_4, ZnO and g-C_3N_4/ZnO. It can be seen that the absorption edge of pure ZnO is about 390 nm, and it has absorption only in the ultraviolet region, while the absorption wavelength of g-C_3N_4 can be expanded to the visible region. After the heterojunction formed, the absorption wavelength has a red shift compared with ZnO, which indicated that the response of ZnO and g-C_3N_4 to the visible region is increased. The Eg of the samples are estimated according to the Tauc equation. As show in Fig. 3(b), the band gap of g-C_3N_4/ZnO decreased compared with ZnO, which improves the absorption efficiency of visible light. Among them, the g-C_3N_4/ZnO composite with a mass ratio of 25% has the smallest band gap, the widest spectral response range and the highest utilization of visible light, so the sample shows the best photocatalytic performance.

Fig. 4 shows the N_2 adsorption-desorption isothermal curves of ZnO, g-C_3N_4 and g-C_3N_4/ZnO. The BET specific surface areas of ZnO, g-C_3N_4 and 25% g-C_3N_4/ZnO are 13.06 m^2/g, 5.87 m^2/g, and 34.3 m^2/g respectively. The specific surface area of g-C_3N_4/ZnO increased significantly after compounded. The pore size distribution of ZnO is mainly distributed in the range of 1.0-3.0 nm, while g-C_3N_4 have a wide pore size distribution from 1 to 159.3 nm, 25% g-C_3N_4/ZnO have lager pore size than ZnO, in which the most pore size is 3.94 nm.

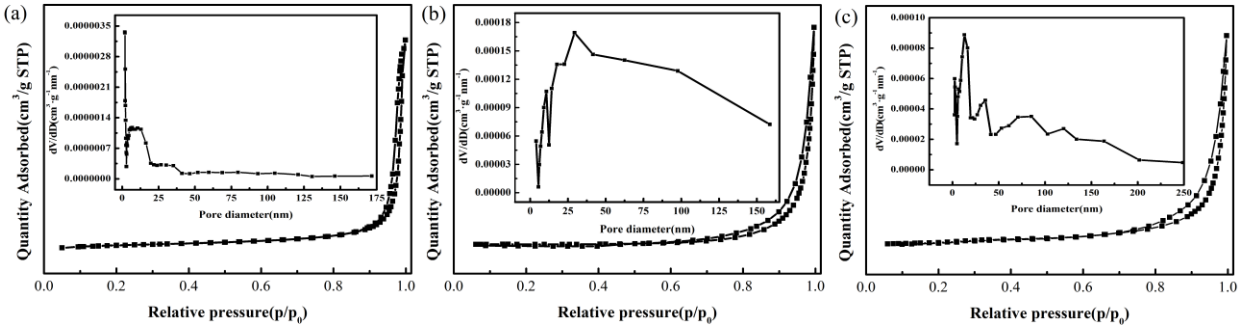

Fig.4 N_2 adsorption-desorption isotherm and Pore size distribution curve (illustration) of ZnO (a); g-C_3N_4 (b) and 25% g-C_3N_4/ZnO (c).

Fig. 5 shows the performance of g-C_3N_4 and g-C_3N_4/ZnO composites photocatalysts of hydrogen under visible light. As can be seen from the figure, compared with g-C_3N_4, the photocatalytic hydrogen production activity of g-C_3N_4/ZnO significantly increased with the increase of the composite ratio, and 25% g-C_3N_4/ZnO has the highest average hydrogen production rate of 306.25 $\mu mol \cdot g^{-1}h^{-1}$, which is 4.6 times higher than of g-C_3N_4.

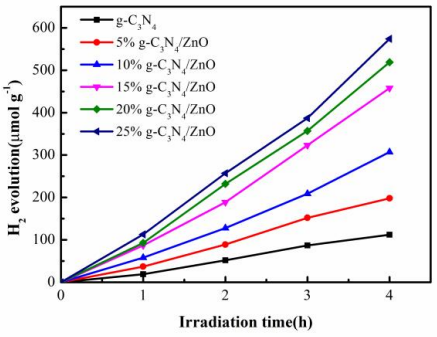

Fig.5 Photocatalytic H_2 evolution rate of g-C_3N_4 and g-C_3N_4/ZnO.

4 Conclusion

By means of composite modification, ZnO was successfully attached to g-C_3N_4, and the electrons in the conduction band of g-C_3N_4 could be easily injected into the conduction band of ZnO, which effectively separated the electron-hole pairs and improved photocatalytic activity of g-C_3N_4. The composites of g-C_3N_4 and ZnO expands the light response range of ZnO semiconductors, and the absorption band edge of g-C_3N_4/ZnO composites is in the visible region. Among them, 25% g-C_3N_4/ZnO composites have the smallest band gap, which improves the utilization of visible light. Therefore, the sample exhibit the best performance of hydrogen production. Under visible light irradiation, the average hydrogen production rate is 306.25 $\mu mol \cdot g^{-1}h^{-1}$, which is 4.6 times higher than that of g-C_3N_4.

References

1. Matsuoka, M., Kitano, M., Takeuchi, M., et al. (2007) Photocatalysis for new energy production: Recent advances in photocatalytic water splitting reactions for hydrogen production. Catalysis Today, 122: 51-61.
2. Zhang, Q.F., Chou, T.P., Russo, B., et al. (2008) Aggregation of ZnO nanocrystallites for high conversion efficiency in dye-sensitized solar cells. Angew Chem. Int. Ed., 47: 2402-2406.
3. Cheng, H.M., Chiu, W.H., Lee, C.H., et al. (2008) Formation of branched ZnO nanowires from solvothermal method and dye-sensitized solar cells applications. The Journal of Physical Chemistry C, 112: 16359-16364.
4. Cheng, H.M., Chiu, W.H., Lee, C.H., et al. (2008) Formation of branched ZnO nanowires from solvothermal method and dye-sensitized solar cells applications. The Journal of Physical Chemistry C, 112: 16359－16364.
5. Zhang, X.H., Peng, T.Y., Yu, L.J., et al. (2014) Visible/near-infrared-light-induced H_2 production over g-C_3N_4 co-sensitized by organic dye and zinc phthalocyanine derivative. ACS Catalysis, 5: 504-510.
6. Sturini, M., Speltini, A. F., Maraschi, G., et al. (2017) g-C_3N_4-promoted degradation of ofloxacin antibiotic in natural waters under simulated sunlight. Environmental Science and Pollution Research, 24: 4153-4161.
7. Goettmann, F., Fischer， A., Antonietti, M., et al. (2006) Chemical synthesis of mesoporous carbon nitrides using hard templates and their use as a metal-free catalyst for friedel-crafts reaction of benzene. Angewandte Chemie International Edition, 45: 4467-4471.
8. Simon, M., Aswani, Y., Peng, G., et al. (2014) Dye-sensitized solar cells with 13% efficiency achieved through the molecular engineering of porphyrin sensitizers. Nature Chemistry, 6: 242-247.
9. Zhang, C., Li, Y., Shuai, D.M., et al. (2019) Graphitic carbon nitride (g-C_3N_4) -based photocatalysts for water disinfection and microbial control: a review. Chemosphere, 214: 462-479.
10. Chen, H., Xie, Y., Sun, X., et al. (2015) Efficient charge separation based on type-II g-C_3N_4/TiO_2-B nanowire/tube heterostructure photocatalysts. Dalton Transactions, 44: 13030-13039.
11. Ge, L., Han, C.C., Liu, J. (2011) Novel visible light-induced g-C_3N_4/Bi_2WO_6 composite photocatalysts for efficient degradation of methyl orange. Applied Catalysis B: Environmental, 108: 100-107.
12. Wang, X.C., Maeda, K., Thomas, A., et al. (2009) A metal-free polymeric photocatalyst for hydrogen production from water under visible light. Nature Materials, 8: 76-80.
13. Chen, G., Li, L., Tao, C.Y., et al. (2016) Effects of microwave heating on microstructures and structure properties of the manganese ore. J Alloys Compd, 657: 515.
14. Anas, S., Rahul, S., Babitha, K.B., et al. (2015) Microwave accelerated synthesis of zinc oxide nanoplates and their enhanced photocatalytic activity under UV and solar illuminations. Appl Surf Sci, 355: 98-103.
15. Chu, S., Wang, Y., Guo, Y., et al. (2013) Band structure engineering of carbon nitride: In search of a polymer photocatalyst with high photooxidation property. ACS Catalysis, 3: 912-919 .
16. Fan, H.G., Zhao, X.T., Yang, J.H., et al. (2012) ZnO-graphene composite for photocatalytic degradation of methylene blue dye. Catalysis Communications, 29: 29-34.